A Two-stage Stochastic Collaborative Intertwined Supply Network Design Problem Under Multiple Disruptions

Abstract

An intertwined supply network (ISN) is a set of interconnected supply chains with dynamic structures that efficiently provide products and services to numerous customers. ISNs inherently involve collaboration among several logistics partners, and such collaboration is pivotal in their long-term resiliency under major disruptions. This paper studies a two-stage stochastic network design problem that incorporates three different resilience strategies to design ISNs under a fair collaboration. We consider capacity expansion, capacity sharing, and rerouting as resilience strategies. We consider disruptions to be stochastic and to incorporate two sources of uncertainty: transportation costs and available capacity at facilities. We develop a Monte-Carlo simulation-based algorithm that uses the sample average approximation scheme to generate high quality solutions for our problem. We analyze the robustness and efficiency of the proposed model on a set of instances with up to 117 nodes and six collaborating companies. The value of collaboration on the ISN performance is assessed by a thorough sensitivity analysis of different metrics. In particular, we evaluate the impact of different levels and scales of random disruptions and flexibility on the network performance, which provides insights into the balance between cost and resilience.

Keywords: Resilient supply chains, collaboration, supply chain disruptions, intertwined supply networks, two-stage stochastic programming

1. Introduction

Supply chain design determines strategic decisions to construct a network and involves selecting suppliers, planning facility locations, and allocating products to different facilities and customers. Several quantitative methods have been applied in the last few decades to find optimal supply chain design structures, considering different assumptions and constraints related to demand, capacities, and costs. Today's fast-changing business environment has triggered huge shifts towards globalization, making the role of uncertainty and risk much more crucial in supply network design (Martel and Klibi, 2016; Cordeau et al., 2021). Globalization creates new challenges alongside the opportunities it brings. The number of interconnecting links between companies within a network is increasing through globalization, making supply chains more prone to disruptions in material and product flows (Chen et al., 2013).

Hendricks and Singhal (2005) define disruptions as unplanned and unexpected events that interrupt the flow of materials and products within a supply chain. Recently, the COVID-19 pandemic has caused significant disruptions in all business sectors in terms of raw material availability, lead times, and cost structures, among other things, highlighting the importance of investing in resilient supply chain research and practices. Resilience enables supply chains to be well prepared for disruptions, quickly lessening their effects, recovering from them, and even going on to higher levels of operational performance (Torabi et al., 2015; Ivanov et al., 2016; Hosseini et al., 2019). Although there is an increasing focus on developing concepts and methodologies for resilient supply chains, most of the work has focused on its qualitative aspects (Hosseini et al., 2019). Only limited studies developed quantitative models to analyze the supply chain resilience under disruption events.

Many modern logistics networks can be modeled as a rather complex intertwined supply network (ISN) involving a set of interdependent supply chains that provide products and services essential to society (Ivanov and Dolgui, 2020). Unlike independent supply chains, an ISN involves interconnected supply chains with dynamic structures, meaning that some entities may play multiple roles in the network (see Figure 1). For instance, at the beginning of the COVID-19 pandemic, some suppliers in the automotive industry simultaneously acted as producers of valves for respirators (Aggi, 2020). Despite the increasing attention to study resilient supply chains, resilient ISNs are rarely addressed in the literature.

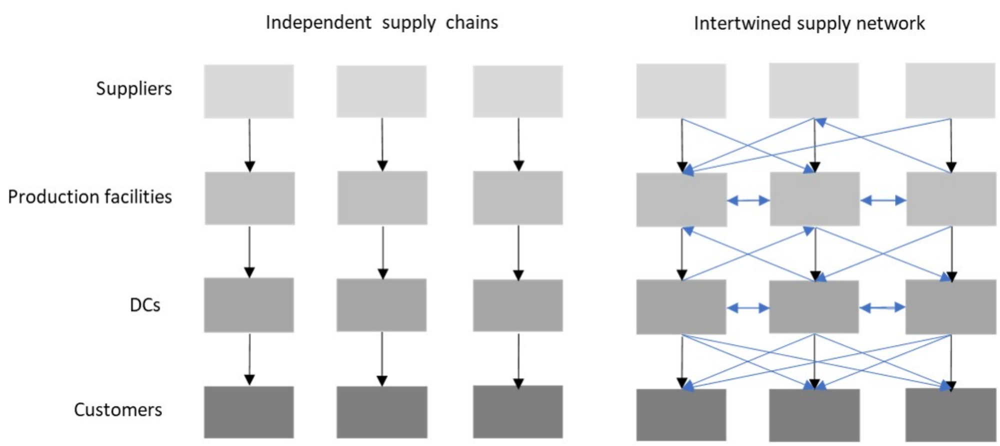

Figure 1: supply chains and intertwined supply networks

When dealing with ISNs, all participants must be resilient to tackle disruptions. Therefore, collaboration among partners plays a crucial role in managing disruptions to operate more efficiently (Duong and Chong, 2020; Shekarian and Mellat Parast, 2020). There are two main types of collaboration studied in logistics networks: vertical and horizontal. Vertical collaboration aims to incorporate suppliers, producers, and distributors to provide the most efficient service to the customer in terms of time, quality, and cost (Cruijssen et al., 2007). Horizontal collaboration is the cooperation between firms that conduct comparable operations at the same level of the supply chain. The combination of vertical and horizontal collaboration is known as lateral collaboration, which is rarely studied in the literature (Simatupang and Sridharan, 2002). It mainly considers the adjustment of inventory and the synchronization of operations from different logistics service providers.

There are strategic, tactical, and operational decisions in collaborative logistics. At the strategic level, participants need to select a coalition. At the tactical level, they have to develop a mechanism to share benefits or costs, whereas at the operational level, they need to decide which resources and in which order to share (Cleophas et al., 2019). They may share resources such as raw materials, transportation vehicles, capacity at manufacturing facilities, distribution centers and warehouses, or exchange customer requests. Many studies in collaborative logistics consider a grand coalition that has the super-additivity property, i.e., the more participants join the collaboration, the more benefit they gain.

In this paper, we introduce a *two-stage stochastic collaborative intertwined supply network design problem* (SCIND) that exploits different resilience strategies to mitigate the negative impact of major uncertain disruptions. Each supply chain within the ISN consists of sets of suppliers, manufacturing facilities, distribution centers, and customers. The uncertainty and risk are represented as disruptions in both the capacities of facilities and the loss of connectivity in the ISN. To mitigate the disruptions, the proposed model simultaneously considers first-stage strategic decisions involving the selection of a set of facilities requiring a capacity expansion and second-stage tactical decisions such as multi-product rerouting and lateral collaboration in the form of crossover capacity sharing of facilities at any level of the network among partners. To the best of our knowledge, this work is the first to study this important form of collaboration in the resilient supply chain design literature. We assume a grand coalition has already been formed, satisfying the super-additivity property. Therefore, the remaining decisions that need to be made at the tactical and operational levels are identifying a fair mechanism for sharing resources and allocating costs among participants. We use a Monte-Carlo simulation-based method, known as the sample average approximation (SAA) scheme (Kleywegt et al., 2002), to solve SCIND problems where capacities at facilities and road accessibility are stochastic parameters with known distributions. We present extensive computational experiments to analyze the robustness of the solutions and efficiency of the proposed model. To this end, the role of collaboration in the network's performance is quantitatively assessed using metrics associated with different resilience strategies.

The remainder of this paper is organized as follows. Section 2 reviews the literature on resilient supply network design problems from different viewpoints. In Section 3, a formal description of the problem and a two-stage stochastic program is given. Section 4 describes our solution method for the SCIND. The results of computational experiments are discussed in Section 5 and, finally, we draw concluding remarks in Section 6.

2. Literature Review

In this section, we review three different aspects of resilient interconnected supply network design under collaboration. We first review resilient supply chain design models under disruptions. We then provide a succinct review of the most related studies on collaborative supply chain design. This followed by a summary of the limited work studying collaboration mechanisms in resilient supply networks. Finally, we highlight the main contributions of our work in view of existing studies.

2.1. *Resilient Supply Chains*

Resilience in supply chains has drawn increased attention in the last decade (Pettit et al., 2013; Hosseini et al., 2019; Goldbeck et al., 2020), in particular on the disruption effects in supply chain network design (Klibi et al., 2010; Hasani and Khosrojerdi, 2016; Govindan et al., 2017). Supply chains are becoming more complex, driven by the trend of globalization, which makes all the business partners in the network vulnerable to disruptions at any level of the network (Li et al., 2020). Hence, it is critical for supply networks to respond quickly and recover from unplanned and unexpected events (Fattahi et al., 2017). The majority of existing research on resilient supply chains is qualitative. Christopher and Peck (2004) investigate different risks incorporated in resilient supply chain design. They underline general principles, including agility and flexibility, as two main elements of resilience. Craighead et al. (2007) state that the severity level of disruption significantly depends on the complexity and density of a supply chain and node criticality. Snyder et al. (2016) discuss the two main approaches in resilience strategies: proactive and reactive. Proactive strategies are protecting policies without any recovery consideration in the presence of a disruption, while reactive policies focus on improving the supply chain process where a disruption has occurred.

Alongside the qualitative studies reviewed above, a few models quantitatively assess the impact of resilience strategies in supply chain design. Torabi et al. (2015) study resilient supplier selection incorporating some proactive strategies, including supplier fortification, backup suppliers, and considering continuity plans to investigate the impact of disruptive incidents on supplier selection. They quantitatively evaluate the robustness and speed of the supply chain by calculating the amount of demand loss without considering resilience strategies and the recovery time needed for full recovery, meeting all demand. Klibi and Martel (2012) propose a stochastic resilient supply chain network design problem. They suggest different distribution strategies to enhance the resilience ability of the network against disruptions in requested arrival time, demand, and facilities capacity. Miller-Hooks et al. (2012) present a two-stage stochastic integer program to quantify the resilience ability of freight transportation logistics in which the proactive decisions are considered in the first stage, while the recovery decisions are made in the second stage. Both types of actions affect the arc capacities and travel time. Azad et al. (2014) develop a stochastic supply chain network design considering disruptions in capacity of distribution centers and transportation modes. They consider that a distribution center may lose a portion of its capacity instead of completely failing under a disruption. They analyze the effect of disruption probability on design decisions. They show that the number of opened facilities and utilization of a safe transportation mode increases when the disruption probability increases.

Cardoso et al. (2015) propose a multi-product multi-period model to design a supply chain under demand uncertainty. They consider different operational and design indicators to analyze resiliency in supply chains. These indicators include node and flow complexity, density, and node criticality. Kim et al. (2015) study different supply chain network structures under disruption using graph theory to assess the resilience level of networks. The result shows that the structural relationships between network entities significantly affect its resilience ability at the holistic level. They argue that a disruption in a node or arc might cause a major failure in the whole network, while there are other nodes or arcs whose loss may not lead to a network-level disruption because of the way they are configured in the network. Therefore, the resilience strategies for a network must be developed at a holistic level rather than an individual entity level. Goldbeck et al. (2020) propose a multi-stage stochastic programming model for the multi-period resilient supply chain planning problem, determining optimal capacity plans, as well as optimal operational adjustments and allocation of repair resources. The authors consider disruptions as interdependent failure incidents that have a ripple effect on the whole supply chain due to failure propagation and functional dependency. They evaluate the network resilience according to a resilience loss triangle metric related to the amount of satisfied demand. The results show that sharing resources improves the supply chain performance in terms of resilience ability as well as resource utilization under interdependent disruption events. Gholami-Zanjani et al. (2020) present a two-stage stochastic problem incorporating resilience strategies to design a food supply network under disruptions in demand, order arrival time, and facility capacities. They apply an algorithm based on Benders decomposition and scenario reduction techniques to solve the proposed model. They assess the effect of resilience strategies, including backup supplier, multiple sourcing, fortification, and capacity expansion, on network design decisions. The results indicate that fortification and backup suppliers bring more resilient solutions against disruptions than the other resilient strategies. We note that, contrary to our work, none of the studies discussed above evaluated the resilience ability of a set of interconnected supply chains. Moreover, they do not incorporate collaboration aspects into the considered resilient supply chain design models.

2.2. Collaborative Supply Chain Design

Existing literature reviews on collaborative logistics problems (see, Verdonck et al., 2016; Cleophas et al., 2019) show that most of the literature can be divided into three categories. The first one, which is the most common one, is sharing the customer orders to efficiently match orders to available transportation resources (Bloos and Kopfer, 2011). The second one is sharing vehicle capacity to minimize transportation cost (Wang et al., 2017), and the last one is sharing storage capacity at distribution centers (Verdonck et al., 2016). Despite the clear benefits of collaborative logistics, cooperation among organizations is practically limited. The main impediment for collaboration among players is designing a fair cost-sharing scheme which mainly falls in the domain of cooperative game theory research in the literature (e.g., Shapley, 1953). Goemans and Skutella (2004) study a collaborative facility location problem using game theory for both public and private facilities to find a fair cost allocation to customers such that there is no coalition of customers that intend to leave. Verdonck et al. (2016) propose a cooperative multi-commodity capacitated facility location model such that distribution centers are fairly shared among carriers to satisfy all demand. They compare three different cost allocation mechanisms: Shapley value, the equal profit method, and the alternative cost avoided method. The results show that the equal profit method finds the most equitable cost allocation among players in the proposed model. Guo et al. (2022) escribes a mixed-integer linear programming model for designing multi-echelon, multi-product supply chains. The authors investigate lateral collaboration in production, distribution, and transportation resources to simultaneously minimize total cost and, sustainability issues, as well as maximize the number of jobs provided by the network in the context of social responsibility. They also propose four cost-sharing mechanisms based on equal-sharing, order-volume, extra-cost, and Shapley value. The mechanisms address how to share the total cost of the network fairly among players. The results of this work show that the collaboration significantly reduces the total cost and carbon emissions. Besides, they find out that among all the cost-sharing mechanisms, the extra-cost strategy ensures that all players acquire cost reduction equitably. However, none of the considered approaches guarantees stability of the collaboration.

According to the literature, most studies have focused on order sharing in a customer-centric context, using cooperative game theory. However, applying game theory often has some downsides, such as its inherent mathematical complexity, stability, and applicability. To the best of our knowledge, Guo et al. (2022) is the only work considering a lateral collaboration at every layer of the supply chain. However, they incorporate different cost-sharing mechanisms that are independent from the collaborative supply chain design decisions since these features are not integrated into the proposed model. Moreover, none of the proposed mechanisms guarantees the stability of collaboration with respect to the cost of each player according to its stand-alone case, i.e., a non-collaborative scenario in which each supply chain operates independently. In this paper we present an integrated centralized cooperative model, driven by the idea of the equal profit method (Frisk et al., 2010, see) for a resilient ISN design problem. It incorporates a mechanism for finding a stable collaboration that minimizes the maximum relative difference in cost-saving and demand satisfaction among all pairs of partners with respect to their stand-alone cases.

2.3. Collaboration in Resilient Supply Chain Networks

Collaboration is one of the primary strategic responses to tackle disruptions in a supply chain network (Duong and Chong, 2020). Cao et al. (2010) discuss the nature and characteristics of collaboration in supply chains such as resource and information sharing, collaborative communication, mutual knowledge creation and decisions, among all supply network participants. Brusset and Teller (2017) examine the resilience level of disrupted supply chains. They conclude that collaborative strategies such as continuous inventory adjustment and sharing information regarding demand forecasting improve the resilience level of a supply chain significantly. Ivanov and Dolgui (2020) introduce the new concept of viability in intertwined supply networks. They apply a dynamic game theory model for a biological system representing an ISN to elaborate on the integrity of collaboration in holistic supply chain networks and survivability under pandemic events. However, none of the studies quantitatively assess the role of collaboration on the resilience ability of ISN.

2.4. Contributions of This Paper

Despite the significant focus on the role of collaboration in the literature, there exists a gap in investigating how collaboration affects supply chain response and recovery from disruptions and how partners in a supply chain network collaborate under disruptions. Therefore, this paper makes three contributions to the supply chain literature. To the best of our knowledge, our work is the first to quantitatively assess the effects of collaboration between partners in a resilient ISN, incorporating capacity sharing, rerouting, and capacity expansion strategies towards managing disruptions. Moreover, it is the first study to consider lateral collaboration in the form of facility capacity sharing at all levels of the resilient supply chain. Most of the literature on resilient supply chains focuses on the resilience ability of individual entities instead of considering resilience from a compound network perspective. Finally, this study investigates the network's resilience at the holistic level with dynamic interactions within the ISN.

3. Problem Definition and Mathematical Models

The SCIND is formally defined as follows. Let M be the set of companies (members of a coalition), K be the set of customer zones, and P be the set of products to produce. Let $G = (V, A)$ be a directed graph, such that the node set V comprises four sets of nodes for each member $m \in M$, including S_m, I_m, J_m, and K representing their set of suppliers, production facilities, distribution centers, and customer zones, respectively. We define $S = \bigcup_{m \in M} S_m$, $I = \bigcup_{m \in M} I_m$ and $J = \bigcup_{m \in M} J_m$. The arc set A comprises three sets of links for each node $i \in S \cup I \cup J$, including A_i^1 representing the set of arcs connecting two nodes in consecutive levels of the same supply chain, and A_i^2 and A_i^3 representing the sets of arcs connecting two nodes of the same level and at different levels of different supply chains, respectively. We assume that direct shipments between nodes in non-consecutive echelons are not allowed (e.g., from supply nodes to distribution centers). Moreover, A_i^+ and A_i^- represent the in-cut and out-cut sets of node i, respectively.

For each $k \in K$ and $p \in P$, we denote by d_k^p the deterministic demand of product p for customer zone k. When demand cannot be met, we incur a unit penalty cost λ^p for each product $p \in P$. We assume that the capacities $\tau_i(\xi)$ of suppliers, manufacturing facilities, and distribution centers $i \in S \cup I \cup J$ to be random variables with known probability distribution representing the future available capacity after a disruption occurs for realization ξ. The capacity of a production facility or distribution center $i \cup I \cup J$ can be increased by the deterministic parameter T_i, when a fixed charge cost f_i is incurred. It is assumed that products consume different amounts of capacity at different facilities. The deterministic unit capacity consumption rate of product $p \in P$ in facility $i \in S \cup I \cup J$ is denoted by r_i^p. Without loss of generality, we assume that each facility can produce or store products of other companies. Whenever it is not possible to produce or operate a product in a facility, its capacity consumption rate can be set to a value larger than the capacity of that facility.

The loss of connectivity between two nodes in the ISN can be caused by either a disruption in road accessibility or a complete failure in the operation of a facility node. We assume that there exist virtual routes with higher transportation costs as the alternative routes between node pairs. Therefore, if a link is disrupted, a node pair's connection might be yet accessible through a virtual route with a higher cost. However, there might be a complete loss of connectivity between some node pairs due to either a lack of alternative transportation routes or due to one of the end nodes becoming non-operational. Arc failures can be modeled implicitly by defining for each arc $a \in A$, a random variable $c_a^p(\xi)$ with known probability distribution denoting the unit transportation costs of product $p \in P$ on arc $a \in A$ for realization ξ.

Given the opportunity of collaboration and a set of manufacturing and distribution centers where capacity can be expanded, the first-stage model decides on capacity expansion of facilities and the maximum percentage of available capacity that companies will share with others when a disruption occurs. According to the realized uncertain scenario and the first-stage information, the second-stage determines the flow of products from suppliers to customers in an optimal form based on a fair collaboration regarding the amount of capacity to be shared with others. These decisions are made such that the following objectives are simultaneously optimized: i) minimize the total cost of the coalition under any disruptive scenario, ii) maximize the fairness between companies by comparing their performance improvement under collaboration with respect to their stand-alone case, and iii) maximize the resilience performance by maximizing the difference in unmet demand for each company compared to its stand-alone case. Accordingly, to evaluate the second and third objectives of SCIND, it is necessary to first obtain an optimal (or approximate) solution to the non-collaborative two-stage stochastic supply chain design problem (SSCD), which corresponds to the stand-alone case of each company when operating independently.

3.1. A Two-stage Stochastic Non-collaborative Supply Chain Design Model

We consider the SSCD in which the capacity of facilities and the transportation costs are uncertain for each coalition member as they operate independently. Let $(\tau(\xi), c(\xi))$ represent the random data vector of capacities and transportation costs and Ξ denote the support of ξ. It is assumed that $\tau_i(\xi)$ and $c_a^p(\xi)$ are independent random variables with known probability distribution functions. Let $G_m = (V_m, A_m)$ be a subgraph of G representing the supply chain of company $m \in M$. It comprises subsets of nodes V_m and arcs A_m of G. The arc set A_m comprises two sets of arcs for each node $i \in S_m \cup I_m \cup J_m$, including A^1_{mi} representing the set of arcs connecting two nodes in consecutive levels of the supply chain, and A^2_{mi} representing the set of arcs connecting two nodes of the same level of the supply chain. The SSCD for each coalition member $m \in M$ can be formulated as a two-stage stochastic program with recourse, where the binary variables y_i are the first-stage decision variables, denoting the decisions on capacity expansion of facility $i \in S_m \cup I_m \cup J_m$. The second-stage decisions consist of routing and demand satisfaction decisions. For each product $p \in P_m$ and arc $a \in A_m$, we define the continuous variable $z_a^p(\xi)$ equal to the portion of product p routed on arc a for realization ξ. For each product $p \in P_m$ in customer zone k, we define the continuous variable $w_k^p(\xi)$ equal to the amount of unsatisfied demand of product p in customer zone k for realization ξ. Using these sets of decision variables, the SSCD for each member $m \in M$ can be stated as follows:

$$\text{minimize} \quad \sum_{i \in J_m \cup I_m} f_i y_i + \mathbb{E}_\xi[\varphi_m(y, \xi)] \tag{1}$$

$$\text{subject to} \quad y_i \in \{0, 1\} \qquad i \in I_m \cup J_m, \tag{2}$$

where $\mathbb{E}_\xi[\varphi_m(y,\xi)]$ is the recourse function and $\mathbb{E}_\xi$ denotes the mathematical expectation with respect to ξ. For a given $\xi \in \Xi$ and fixed first-stage vector (y) satisfying constraints (2), we have

$$\varphi_m(y,\xi) = \text{minimize} \quad \sum_{a\in A_m}\sum_{p\in P_m} c_a^p(\xi) z_a^p(\xi) + \sum_{k\in K}\sum_{p\in P_m} \lambda^p w_k^p(\xi) \tag{3}$$

$$\text{subject to} \quad \sum_{p\in P}\sum_{a\in A_{mi}^1} r_{ip} z_a^p(\xi) \leqslant \tau_i(\xi) \qquad i \in S_m \tag{4}$$

$$\sum_{a\in A_{mi}^+} z_a^p(\xi) - \sum_{a\in A_{mi}^-} z_a^p(\xi) = 0 \qquad p \in P_m, i \in I_m \cup J_m \tag{5}$$

$$\sum_{p\in P_m} r_{ip}\left(\sum_{a\in A_{mi}^-} z_a^p(\xi) - \sum_{a\in A_{mi}^{2+}} z_a^p(\xi)\right) \leqslant \tau_i(\xi) + T_i y_i \qquad i \in I_m \tag{6}$$

$$\sum_{a\in A_{mi}^-}\sum_{p\in P_m} r_{ip} z_a^p(\xi) \leqslant \tau_i(\xi) + T_i y_i \qquad i \in J_m \tag{7}$$

$$\sum_{a\in A_{mk}^+} z_a^p(\xi) + w_k^p(\xi) = d_k^p \qquad p \in P_m, k \in K \tag{8}$$

$$z_a^p(\xi) \geqslant 0 \qquad p \in P_m, a \in A_m \tag{9}$$

$$w_k^p(\xi) \geqslant 0 \qquad p \in P_m, k \in K. \tag{10}$$

The objective function (1) minimizes the total cost of the supply chain of company $m \in M$, including the total capacity expansion cost of facilities and the expected cost of transportation and unsatisfied demand. Constraints (4) ensure the total flow from each supplier does not exceed its available capacity. Constraints (5) correspond to the flow conservation on arcs in the second and third layers of the supply chain (manufacturing facility and distribution center nodes). Constraints (6) guarantee that the total flow from a manufacturing facility does not exceed its available production capacity. It is assumed that if an order is physically processed by a manufacturer and then shipped to another manufacturing facility to be transferred to a distribution center, that order does not consume the production capacity of the second facility. Constraints (7) ensure the total amount of products shipped via a distribution center does not exceed its available capacity. Constraints (8) determine the unsatisfied demand.

3.2. A Two-stage Stochastic Collaborative Intertwined Supply Network Design Model

The SCIND can be formulated as a two-stage stochastic program with recourse, where the binary variables y_i and continuous variables q_i are the first-stage decision variables, denoting the decisions on capacity expansion of facility $i \in S \cup I \cup J$, and the maximum capacity percentage of facility $i \in S_m \cup I_m \cup J_m$ that company $m \in M$ will share with other members of the coalition in the future, respectively. The second-stage decisions consist of routing and demand satisfaction decisions for each product under a fair collaboration.

We now describe the three objectives of the SCIND problem. The first objective is the total cost of the coalition under disruptive scenario ξ and is formally defined as follows:

$$g^1(z,w,\xi) = \sum_{a\in A}\sum_{p\in P} c_a^p(\xi) z_a^p(\xi) + \sum_{k\in K}\sum_{p\in P} \lambda_p w_k^p(\xi).$$

The second objective corresponds to the maximum relative difference in cost between all companies for each realization ξ. Let $\hat{y}_{im}$ be the value of the optimal first-stage solution of the SSCD problem (1)–(2), and $\bar{z}_{am}^p(\xi)$ and $\bar{w}_{km}^p(\xi)$ be the optimal solution of the second-stage problem of the SSCD (3)–(10) associated with the supply chain of company $m \in M$ that performs independently under the particular realization ξ. Let $TC_m(\xi)$ be the total cost of company $m \in M$ under realization ξ in the stand-alone case, which is defined as

$$TC_m(\xi) = \sum_{i\in I_m \cup J_m} f_i \hat{y}_i + \sum_{a\in A}\sum_{p\in P_m} c_a^p(\xi)\bar{z}_{am}^p(\xi).$$

Given $TC_m(\xi)$, the second objective can be stated as:

$$g^2(z,w,\xi) = \max_{m,m'\in M, m\neq m'} \left\{ \frac{\sum\limits_{i\in I_m\cup J_m} f_i y_i + \sum\limits_{a\in A}\sum\limits_{p\in P_m} c_a^p(\xi) z_a^p(\xi)}{TC_m(\xi)} - \frac{\sum\limits_{i\in I_{m'}\cup J_{m'}} f_i y_{im} + \sum\limits_{a\in A}\sum\limits_{p\in P_{m'}} c_a^p(\xi) z_a^p(\xi)}{TC_{m'}(\xi)} \right\}.$$

The third objective represents the maximum relative difference in unmet demand between all companies for each realization ξ. Let $\Lambda_m(\xi)$ be the total unmet demand cost of company $m \in M$ for realization ξ under stand-alone case. It is defined as

$$\Lambda_m(\xi) = \sum_{k\in K}\sum_{p\in P_m} C_p \bar{w}_{km}^p(\xi).$$

Given $\Lambda_m(\xi)$, the third objective can be stated as

$$g^3(z,w,\xi) = \max_{m,m'\in M, m\neq m'} \left\{ \frac{\sum\limits_{k\in K}\sum\limits_{p\in P_m} C_p w_k^p(\xi)}{\Lambda_m(\xi)} - \frac{\sum\limits_{k\in K}\sum\limits_{p\in P_{m'}} C_p w_k^p(\xi)}{\Lambda_{m'}(\xi)} \right\}.$$

The last objective relates to the network resilience ability from an operational perspective. It is computed as the difference in unsatisfied demand by each company compared to its stand-alone case. Minimizing the difference leads to satisfying the demand as much as possible under a disruption. Besides, it guarantees the coalition's stability in the sense that there is no member in the coalition that satisfies its demand less than in the stand-alone case. Given $\Lambda_m(\xi)$, the fourth objective can be defined as:

$$g^4(z,w,\xi) = \sum_{m\in M}\left(\sum_{k\in K}\sum_{p\in P_m} \lambda_p w_k^p(\xi) - \Lambda_m(\xi) \right).$$

Using all sets of decisions variables and parameters discussed above, the SCIND can be stated as:

$$\text{minimize} \qquad \theta_1 \sum_{i\in J\cup I} f_i y_i + \mathbb{E}_\xi[Q(y,q,\xi)] \tag{11}$$

$$\text{subject to} \quad 0 \leqslant q_i \leqslant 1 \qquad i \in S \cup I \cup J \tag{12}$$

$$y_i \in \{0,1\} \qquad i \in I \cup J, \tag{13}$$

where $\mathbb{E}_\xi[Q(y,q,\xi)]$ is the recourse function with respect to ξ. For a given $\xi \in \Xi$ and fixed first-stage vector (q,y) satisfying constraints (12)–(13), we have

$$Q(y,q,\xi) = \text{minimize} \quad \theta_1 g^1(z,w,\xi) + \theta_2 g^2(z,w,\xi) + \theta_3 g^3(z,w,\xi) + \theta_4 g^4(z,w,\xi) \tag{14}$$

$$\text{subject to} \quad \sum_{p\in P} \sum_{a\in A_{i1}\cup A_{i3}} r_{ip} z_a^p(\xi) \leqslant \tau_i(\xi) \qquad i \in S, \tag{15}$$

$$\sum_{p\in P\backslash P_m} \sum_{a\in A_{i1}\cup A_{i3}} r_{ip} z_a^p(\xi) \leqslant \tau_i(\xi) q_i \qquad i \in S_m, m \in M \tag{16}$$

$$\sum_{a\in A_i^+} z_a^p(\xi) - \sum_{l\in A_i^-} z_a^p(\xi) = 0 \qquad p \in P, i \in I \cup J \tag{17}$$

$$\sum_{p\in P} r_{ip} \left(\sum_{a\in A_i^-} z_a^p(\xi) - \sum_{a\in A_{i2}^+} z_a^p(\xi) \right) \leqslant \tau_i(\xi) + T_i y_i \qquad i \in I \tag{18}$$

$$\sum_{p\in P\backslash P_m} r_{ip} \left(\sum_{a\in A_i^-} z_a^p(\xi) - \sum_{a\in A_{i2}^+} z_a^p(\xi) \right) \leqslant (\tau_i(\xi) + T_i y_i)\, q_i \qquad i \in I_m, m \in M \tag{19}$$

$$\sum_{a\in A_i^-} \sum_{p\in P} r_{ip} z_a^p(\xi) \leqslant \tau_i(\xi) + T_i y_i \qquad i \in J \tag{20}$$

$$\sum_{a\in A_i^-} \sum_{p\in P\backslash P_m} r_{ip} z_a^p(\xi) \leqslant (\tau_i(\xi) + T_i y_i) q_i \qquad i \in J_m, m \in M \tag{21}$$

$$\sum_{a\in A_k^+} z_a^p(\xi) + w_k^p(\xi) = d_k^p \qquad p \in P, k \in K \tag{22}$$

$$z_a^p(\xi) \geqslant 0 \qquad p \in P, a \in A \tag{23}$$

$$w_k^p(\xi) \geqslant 0 \qquad p \in P, k \in K. \tag{24}$$

The objective function (14) minimizes the weighted sum of the four objectives. The interpretation of constraints (15), (17), (18), (20), and (22) is the same as that of constraints (4)–(8), respectively. Constraints (16), (19), and (21) ensure that the total items shared with other players do not exceed the maximum sharing capacity assigned in each supplier, manufacturing facility, and distribution center, respectively. Since constraints (19) and (21) are nonlinear, the following equivalent linear constraints are used instead, where B denotes a very large number:

$$\sum_{p\in P\backslash P_m} r_{ip} \left(\sum_{a\in A_i^-} z_a^p(\xi) - \sum_{a\in A_{i2}^+} z_a^p(\xi) \right) \leqslant \tau_i(\xi) q_i + B y_i \qquad i \in I_m, m \in M \tag{25}$$

$$\sum_{p \in P \setminus P_m} r_{ip} \left(\sum_{a \in A_i^-} z_a^p(\xi) - \sum_{l \in L_{i2}^+} z_a^p(\xi) \right) \leqslant (\tau_i(\xi) + T_i) q_i + B(1 - y_i) \qquad i \in I_m, m \in M \tag{26}$$

$$\sum_{a \in A_i^-} \sum_{p \in P \setminus P_c} r_{ip} z_a^p(\xi) \leqslant \tau_i(\xi) q_i + B y_i \qquad i \in J_m, m \in M \tag{27}$$

$$\sum_{a \in A_i^-} \sum_{p \in P \setminus P_m} r_{ip} z_a^p(\xi) \leqslant (\tau_i(\xi) + T_i) q_i + B(1 - y_i) \qquad i \in J_m, m \in M. \tag{28}$$

4. Algorithm for the SCIND

In this section, we present a Monte-Carlo simulation technique based on the sample average approximation (SAA) scheme (Shapiro and Homem-de Mello, 1998; Mak et al., 1999) to solve the SCIND. From the stochastic supply chain design literature, we note that the SAA scheme is an efficient algorithm that has been successfully used to obtain high-quality solutions for complex stochastic problems (see for instance, Santoso et al., 2005; Contreras et al., 2011; Martel and Klibi, 2016, and references therein). The SAA scheme relies on the idea of generating a large number of random scenarios and estimating the expected value function using the associated sample average function. A candidate solution to the SCIND is then constructed by solving a deterministic optimization problem.

In the SAA scheme, a random sample $N = \{\xi^1, ..., \xi^{|N|}\}$ of realizations of the random vector ξ is generated, and the second-stage expectation $\mathbb{E}_\xi[Q(y, q, \xi)]$ is approximated by the sample average function

$$\frac{1}{N} \sum_{n \in N} \left(\theta_1 g^1(z, w, \xi^n) + \theta_2 g^2(z, w, \xi^n) + \theta_3 g^3(z, w, \xi^n) + \theta_4 g^4(z, w, \xi^n) \right).$$

Therefore, the original problem is approximated by the SAA problem:

$$\text{minimize} \quad \theta_1 \sum_{i \in J \cup I} f_i y_i + \frac{1}{N} \sum_{n \in N} \left(\theta_1 g^1(z, w, \xi^n) + \theta_2 g^2(z, w, \xi^n) + \theta_3 g^3(z, w, \xi^n) + \theta_4 g^4(z, w, \xi^n) \right) \tag{29}$$

$$\text{subject to} \quad \sum_{p \in P} \sum_{a \in A_{i1} \cup A_{i3}} r_{ip} z_a^{pn} \leqslant \tau_i^n \qquad i \in S, n \in N \tag{30}$$

$$\sum_{p \in P \setminus P_m} \sum_{a \in A_{i1} \cup A_{i3}} r_{ip} z_a^{pn} \leqslant \tau_i^n q_i \qquad i \in S_m, m \in M, n \in N \tag{31}$$

$$\sum_{a \in A_i^+} z_a^{pn} - \sum_{a \in A_i^-} z_a^{pn} = 0 \qquad p \in P, i \in I \cup J, n \in N \tag{32}$$

$$\sum_{p \in P} r_{ip} \left(\sum_{a \in A_i^-} z_a^{pn} - \sum_{a \in A_{i2}^+} z_a^{pn} \right) \leqslant \tau_i^n + T_i y_i \qquad i \in I, n \in N \tag{33}$$

$$\sum_{p \in P \setminus P_m} r_{ip} \left(\sum_{a \in A_i^-} z_a^{pn} - \sum_{a \in A_{i2}^+} z_a^{pn} \right) \leqslant (\tau_i^n + T_i y_i)\, q_i \qquad i \in I_m, m \in M, n \in N \tag{34}$$

$$\sum_{a \in A_i^-} \sum_{p \in P} r_{ip} z_a^{pn} \leqslant \tau_i^n + T_i y_i \qquad i \in J, n \in N \tag{35}$$

$$\sum_{l \in A_i^-} \sum_{p \in P \setminus P_m} r_{ip} z_a^{pn} \leqslant (\tau_i^n + T_i y_i) q_i \qquad i \in J_m, m \in M, n \in N \tag{36}$$

$$\sum_{a \in A_k^+} z_a^{pn} + w_k^{pn} = d_k^p \qquad p \in P, k \in K, n \in N \tag{37}$$

$$z_a^{pn} \geqslant 0 \qquad p \in P, a \in A, n \in N \tag{38}$$

$$w_k^{pn} \geqslant 0 \qquad p \in P, k \in K, n \in N \tag{39}$$

$$0 \leqslant q_i \leqslant 1 \qquad i \in S \cup I \cup J \tag{40}$$

$$y_i \in \{0, 1\} \qquad i \in I \cup J, \tag{41}$$

where C_a^{pn} and τ_i^n denote the realization of the uncertain parameters of scenario n, and z_a^{pn} and w_k^{pn} the value of the decision variables of scenario $n \in N$. Given that $g^2(z, w, \xi^n)$ and $g^3(z, w, \xi^n)$ are nonlinear functions, the following constraints are used to linearize them:

$$\eta_{cost}^n \geqslant \frac{\sum_{i \in I_m \cup J_m} f_i y_i + \sum_{a \in A} \sum_{p \in P_m} c_a^{pn} z_a^{pn}}{TC_m^n} - \frac{\sum_{i \in I_{m'} \cup J_{m'}} f_i y_i + \sum_{a \in A} \sum_{p \in P_{m'}} c_a^{pn} z_a^{pn}}{TC_{m'}^n} \qquad m, m' \in M, m \neq m', n \in N \tag{42}$$

$$\eta_{loss}^n \geqslant \frac{\sum_{k \in K} \sum_{p \in P_m} C_p w_k^{pn}}{\Lambda_m^n} - \frac{\sum_{k \in K} \sum_{p \in P_{m'}} C_p w_k^{pn}}{\Lambda_{m'}^n} \qquad m, m' \in M, m \neq m', n \in N, \tag{43}$$

where η_{cost}^n and η_{loss}^n are the maximum relative difference in cost and unmet demand between members of the coalition, respectively. Given that obtaining the optimal values of $TC_m(\xi)$ and $\Lambda_m(\xi)$ involves solving SSCD with the SAA scheme for every company $m \in M$, we approximate these values with TC_m^n and Λ_m^n defined as follows:

$$TC_m^n = \sum_{i \in I_m \cup J_m} f_i \bar{y}_{im}^n + \sum_{a \in A} \sum_{p \in P_m} c_a^{pn} \bar{z}_{am}^{pn} \quad , \qquad \Lambda_m(\xi) = \sum_{k \in K} \sum_{p \in P_m} C_p \bar{w}_{km}^{pn},$$

where $(\bar{y}_{im}^n, \bar{z}_{am}^{pn}, \bar{w}_{km}^{pn})$ is an optimal solution of the first-stage problem of SSCD under the same scenario $n \in N$ considered in the first-stage problem of the SCIND.

Kleywegt et al. (2002) show that under mild regularity conditions, the optimal solution value and the optimal solution converge with probability one to their true counterparts, as the sample size $|N|$ increases. Moreover, the optimal solution converges to an optimal solution of the true problem with probability approaching one exponentially fast. We can estimate the sample size $|N|$ needed to obtain an ϵ-optimal solution to the original problem. However, it is known that such sample size estimate is too conservative for practical applications. Therefore, a less conservative way is to find a trade-off between the quality of the obtained solution and the computational time needed to solve the SAA problem (29)–(43). In this approach, the SAA scheme includes repeated solutions of smaller SAA problems with independent samples rather than solving one large-scale SAA problem. Statistical confidence intervals are then computed on the quality of the estimated solutions. We now describe this procedure. In Section 5, we show how to select a sample size that can produce tight and accurate statistical bounds.

1. Generate a set of independent sample $M = \{N_1, ..., N_{|M|}\}$. For each sample $N_m = \{\xi_m^1, ..., \xi_m^{|N|}\}$, solve the corresponding SAA problem (29)–(43).
2. Let $v^{N_m}, m = 1, ..., |M|$ be the corresponding optimal objective value to the sample $\xi_m^{|N|}$. The average objective value of all optimal solutions and their variance can be computed as follows:

$$\bar{v}_M^N = \frac{1}{|M|} \sum_{m \in M} v^{N_m},$$

$$\sigma^2_{\bar{v}_M^N} = \frac{1}{|M|(|M|-1)} \sum_{m \in M} (v^{N_m} - \bar{v}_M^N)^2.$$

   We note that $\bar{v}_M^N$ is a statistical lower bound for the optimal objective value of the problem (11)–(13), and σ^2 is the estimated variance of the statistical lower bound (Mak et al., 1999).
3. Select a feasible solution $(\bar{y}, \bar{q})$ of the original problem. For instance, we can use one of the obtained solutions $(\hat{y}_N^m, \hat{q}_N^m)$ of the SAA problem (29)–(43) to estimate the true objective function (11) as follows:

$$\hat{v}_{N'}(\bar{y}, \bar{q}) = \theta_1 \sum_{i \in J \cup I} f_i \bar{y}_i + \frac{1}{N'} \sum_{n \in N'} \sum_{e=1}^{4} \theta_e g^e(z^*, w^*, \xi^n),$$

   where $\xi^1, ..., \xi^{N'}$ is a sample of size $|N'|$ generated independently of the sample used in the SAA problem to obtain $\bar{y}$ and $\bar{q}$. Given that the variables of the first stage $(\bar{y}, \bar{q})$ are fixed for each sample, z^* and w^* are the best optimal solution of the second-stage problem among all samples. It is noted that the estimation of the true objective function $(\hat{v}_{N'}(\bar{y}, \bar{q}))$ is an estimate of the upper bound on the optimal solution of the original problem, since the first-stage variables $(\bar{y}, \bar{q})$ used in the second stage are feasible. Assuming the sample $\xi^1, ..., \xi^{N'}$ is independent identically distributed (iid), we can estimate the variance of $\hat{v}_{N'}(\bar{y}, \bar{q})$ as follows:

$$\sigma^2_{N'}(\bar{y}, \bar{q}) = \frac{1}{|N'|(|N'|-1)} \sum_{n \in N'} \left(\theta_1 \sum_{i \in J \cup I} f_i \bar{y}_i + \sum_{e=1}^{4} \theta_e g^e(z^*, w^*, \xi^n) - \hat{v}_{N'}(\bar{y}, \bar{q}) \right)^2.$$

4. The absolute optimality gap of the obtained solution and its variance are calculated according to the lower and upper bound estimations on the optimal objective value of the original problem (11)–(13) computed in steps 2 and 3:

$$gap(\bar{y}, \bar{q}) = \hat{v}_{N'}(\bar{y}, \bar{q}) - \bar{v}_M^N,$$

$$\sigma^2_{gap} = \sigma^2_{N'}(\bar{y}, \bar{q}) + \sigma^2_{\bar{v}_M^N}.$$

5. Computational Experiments

In this section, we present the results of computational experiments to analyze the efficiency and efficacy of the proposed algorithm. We first discuss implementation details concerning the convergence of the SAA algorithm under different continuous probability distributions. We then present an extensive sensitivity analysis of the proposed model to show the effect of different levels of uncertainty and flexibility on the performance of the resilient network under uniform and gamma distributions. Finally, we assess the robustness and challenges of the proposed model on instances with up to 117 nodes and six collaborating companies. These instances are different in terms of the number of nodes, products and companies as shown in Table 1. We considered an incomplete graph representing an intertwined supply network. All formulations and algorithms were coded in C and run on an Intel Xeon E5-2687W v3 processor at 3.10 GHz in a Linux environment. The formulations were implemented using the Callable Library of CPLEX 12.9.

Table 1: Size of instances

Instance size	**1**	**2**	**3**	**4**	**5**
Companies $\lvert M\rvert$	2	3	5	5	6
Suppliers $\lvert S\rvert$	3	5	6	8	9
Producers $\lvert I\rvert$	3	5	6	8	9
DCs $\lvert J\rvert$	3	5	6	8	9
Products $\lvert P\rvert$	6	10	12	16	18
Customers $\lvert K\rvert$	30	50	60	80	90
Nodes	**39**	**65**	**78**	**104**	**117**

5.1. *Description of Data*

We next describe the procedure that is applied to randomly generate different test instances with respect to the deterministic parameters and disruption scenarios.

5.1.1. *Deterministic Parameters*

Different instances are randomly generated using the procedure described in Cordeau et al. (2006). The instances differ in terms of the number of suppliers ($|S|$), the number of production facilities ($|I|$), the number of distribution centers ($|J|$), the number of customers ($|K|$), the number of products ($|P|$), and the number of companies ($|M|$) in the coalition. For a problem with $|K| = n$, the number of suppliers, production facilities, distribution centers, and products of each company is randomly generated such that $|S| = |I| = |J| = \lfloor n/10 \rfloor$ and $|P| = \lfloor n/5 \rfloor$. Since a facility may produce or store products of other companies, we randomly select the facilities that can produce or store each product.

The capacity structure is determined as follows. The unit capacity consumption rate of product $p \in P$ in facility $i \in S \cup I \cup J$ is randomly generated from the integer set $\{1, ..., 15\}$ with a uniform distribution. Let u_m be the total capacity needed to meet the total demand for company $m \in M$, and $|S_m|, |I_m|, |J_m|$ be the number of facilities (suppliers, manufactures, distribution centers) of company $m \in M$. The minimum capacity of each facility is the total capacity divided by the number of facilities owned by each company (i.e., $\bar{u}_{s_m} = u_m/|S_m|$). The initial capacity of a facility ($\overline{\tau}_i$) is randomly selected from the set $[\alpha.\bar{u}, \beta.\bar{u}]$ using a uniform distribution. We assumed that $\alpha = 1$ and $\beta = |S_c| \vee |I_c| \vee |J_c|$.

The cost structure is determined based on a case study discussed by Martel and Klibi (2016). A fixed charge cost ($\bar{f}$) for capacity expansion of each type of facilities (production facilities and distribution centers) is randomly generated in an interval shown in Table 2 using a uniform distribution. Afterwards, the fixed charge cost of each facility is randomly selected from the set $[\alpha.\bar{f}, \beta.\bar{f}]$, where $\alpha = 0.75$ and $\beta = 1.25$, multiplied by $\overline{\tau}_i / \sum_{i \in I} \overline{\tau}_i$. It ensures that the fixed capacity expansion cost of each facility is relative to its size. The original freight cost ($\bar{c}_a^p$) of product $p \in P_m$ on arc $a \in A_1$ is randomly generated using a uniform distribution in an interval shown in Table 2. The freight cost of product $p \in P_m$ on arc $a \in A_2 \cup A_3$ is at most 50% more expensive than the price shown in Table 2, since the origin or the destination of the shipment belongs to another company. The demand of products and the penalty cost of unsatisfied demand are randomly generated in the interval $[10000, 40000]$ and $[60, 150]$ using a uniform distribution, respectively.

Finally, parameters θ_1, θ_2, θ_3, and θ_4 in objective function (29) reflect the weights to scale the values of different objectives to the same level of measurement:

$$\theta_1 = \theta, \qquad \theta_2 = \alpha_1(1-\theta), \qquad \theta_3 = \alpha_2(1-\theta), \qquad \theta_4 = 0.1\theta.$$

Parameters α_1 and α_2 reflect weights to prioritize the fairness in unmet demand cost over the logistic cost (capacity expansion and freight costs). According to the comparison of different solutions we obtained through applying different weights to the multiple objectives, we conclude that $\theta_1 = 0.3$, $\alpha_1 = 10000$, and $\alpha_2 = 200000$ are the most proper weights that help the algorithm find an efficient solution.

5.1.2. Disruption Scenarios Generation

We generate a set of random scenarios $N = \{\xi^i, ..., \xi^{|N|}\}$ as a set of realizations of the random vector ξ for the SAA algorithm. We assume that only a part of the set belongs to disruptive scenarios, which are randomly generated with uniform and gamma distributions. The rest of the set is the same base scenario, a given realization of uncertain data without disruptions. To reduce the computational time, we consider a subset of N, which includes one base scenario along with all disruptive scenarios. Accordingly, we incorporate a random weight in the objective function that is associated with the base scenario. We generate a random number between 0 and 1 using a uniform distribution $|N|$ times, and count the number of times (n_b) that the generated random number is greater than the given disruption probability. The number n_b is the weight of base scenario in the objective function.

The disruption scenarios are generated according to a disruption rate, a random number between 0 and 1 under uniform and gamma distributions that is generated independently for the uncertain capacity and freight cost ($\delta_i(\xi)$/ $\delta_a^p(\xi)$). Recall that we consider disruptions in capacities and road accessibility at any level of the network. From a practical point of view, it is extremely rare to observe a 100% scale of disruption such that all facilities and roads within a network become simultaneously affected by a disruption event. Therefore, we generate a random number between 0 and 1 using a uniform distribution for each facility and arc in the network. If the generated number associated with an entity in the network (node/arc) is less than the given disruption scale (i.e., 20%), that entity is considered to be affected by the disruption scenario. Therefore, we generate the stochastic capacities under uniform and gamma distributions as $((1-\delta_i(\xi)).\overline{\tau}_i)$, and the stochastic freight cost under uniform and gamma distributions as $((1+\delta^p_a(\xi)).\overline{c}^p_a)$ for only the facilities and arcs that are randomly selected to be disrupted under disruption scenario ξ.

Table 2: Freight and facility fixed costs

	Freight Cost					**Fixed Cost**	
	Supplier to Plant	**Plant to Plant**	**Plant to DC**	**DC to DC**	**DC to Customer**	**Plant**	**DC**
Cost Interval ($)	(80, 120)	(10, 60)	(100, 200)	(10, 60)	(20, 45)	(2000000, 4000000)	(1000000, 2000000)

5.2. Practical Convergence of the SAA Algorithm

The goal of the first set of experiments is to assess the practical convergence of the SAA algorithm. We are also interested in determining the proper number of independent samples $|M|$ with size $|N|$ to obtain the most efficient configuration of the algorithm. Recall that as the sample size $|N|$ and number of replications $|M|$ increase, the SAA algorithm provides better feasible solutions with tighter optimality gaps and smaller variance for the corresponding estimate, at the expense of increasing the computational time. Therefore, we seek a trade-off between the quality of the generated solution and computational time such that the algorithm provides a solution with a sufficiently small estimated optimality gap and small variance while the CPU time stays at a minimum. Different combinations of sample size $|N| = \{50, 100, 200, 400\}$ and number of samples $|M| = \{10, 20, 40, 60\}$ are considered to analyze the practical convergence of the SAA algorithm under both uniform and gamma distributions. Besides, a sample size $|N'| = 10000$ is used to find fair estimations of actual optimal solution values. Figures 2 A and B represent the estimated optimality gap for different values of $|N|$ and $|M|$ under uniform and gamma distributions, respectively.

Figure 2 shows that the algorithm provides a more precise estimate of the optimality gap by increasing the number of SAA problems associated with a particular value of sample size $|N|$ for both the uniform and gamma distributions. Figure 2 A indicates that the algorithm with sample size $|N|= 200$ obtains a more accurate optimality gap below 0.1% even with a small number of SAA problems considering uniform distribution. It is also observed that by choosing the sample size $|N|= 100$, an increase on the number of problems $|M|$ is required to obtain an accurate optimality gap below 0.1%. Figure 2 B indicates that by applying sample size $|N|= 200$, a small number of SAA problems are needed to find a solution with an optimality gap below 0.1%. While using the other sample sizes, the optimality gap stays above 0.3%, even if the number of SAA problems is increased.

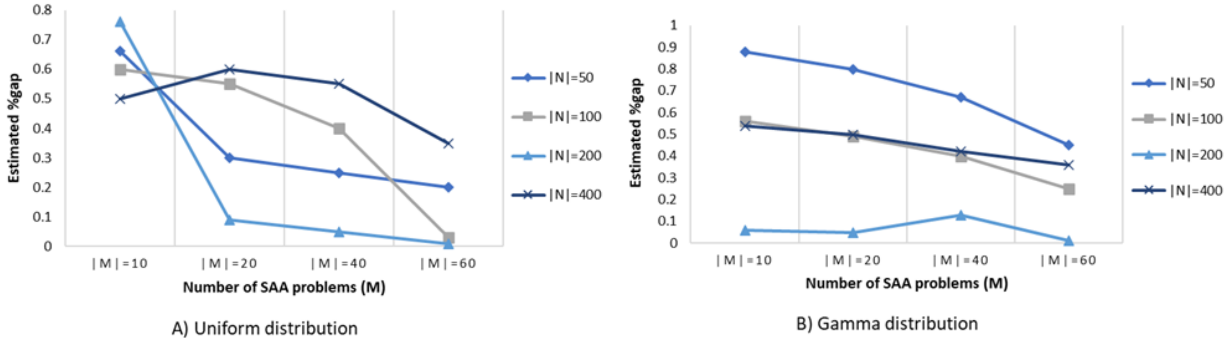

Figure 2: Optimality gap for the instance size 2 with different values of $|N|$ and $|M|$.

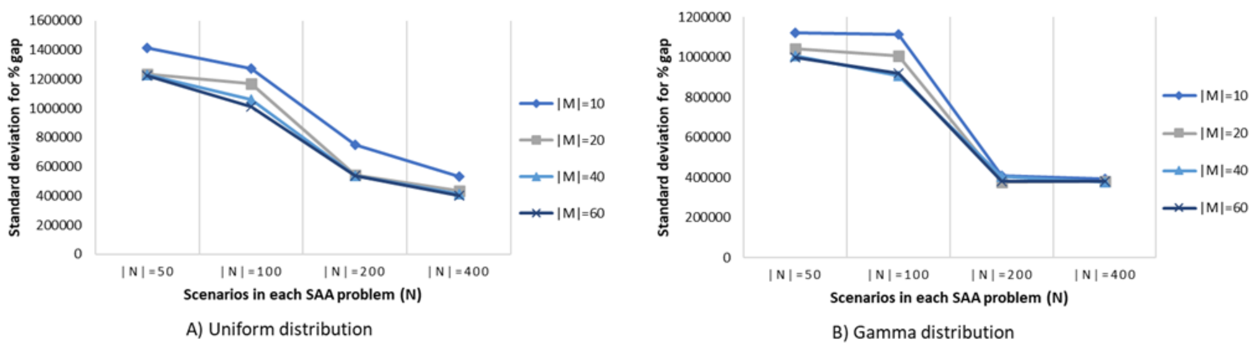

Figure 3: Standard deviation for optimality gap for the instance size 2 with different values of $|N|$ and $|M|$.

Figures 3 A and B show the standard deviation for the optimality gap over different sample sizes $|N|$ and number of replications $|M|$ under uniform and gamma distributions, respectively. These figures indicate that the standard deviation is significantly reduced by increasing the sample size for the uniform and gamma distributions. Besides, we observe that if we choose a large sample size $|N|= 200$ and $|N|= 400$, the standard deviation for the optimality gap is reasonably small for both the uniform and gamma distributions, while for small sample sizes $|N|= 50$ and $|N|= 100$, the standard deviation remains relatively high when the number of SAA problem is increased.

Figures 4 A and B represent the total CPU time spent for solving SAA problems over different values of $|N|$ and $|M|$ under the uniform and gamma distributions, respectively. Both figures show that the CPU time grows when increasing the number of SAA problems $|M|$ and sample size $|N|$. It seems that the computational complexity increased almost linearly in $|N|$ to solve the problems. We note that when we use a large sample size $|N|$, a small number of SAA problems $|M|$ is required to have an accurate optimality gap and a small variance. Therefore, it is more reasonable to increase the size of the sample rather than the number of SAA problems. As a result, sample sizes $|N|= 200$ and $|M|= 20$ are used for the remaining sets of computational experiments.

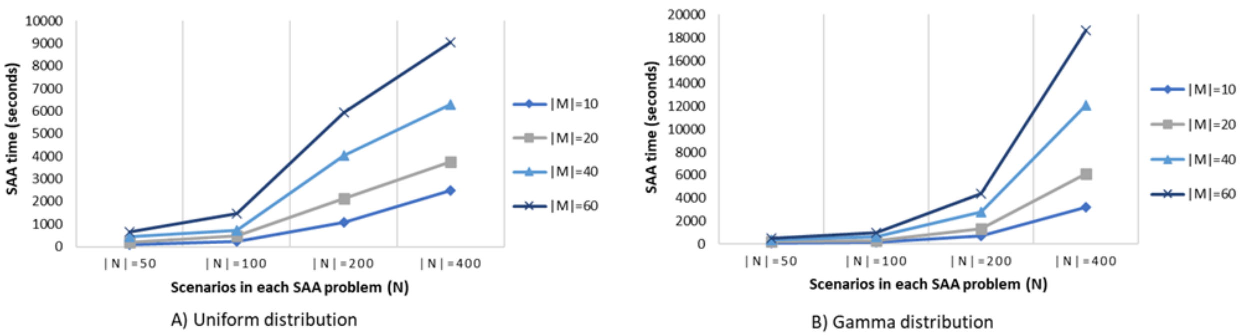

Figure 4: Total CPU time for the instance size 2 with different values of $|N|$ and $|M|$.

5.3. Sensitivity Analysis

In this part of the experiments, we provide the results of a sensitivity analysis of the problem using different disruption scenarios associated with uncertainty in freight cost and capacity of facilities. For these experiments, we employ ten different performance indicators from the literature and evaluate them on different solution networks to assess their behavior when considering different levels of disruption from both design and performance perspectives.

5.3.1. Effects of Disruptions on Resilient Network Performance and Design

Evaluating resilience is a challenging task. Although there have been efforts in the literature to develop different metrics for resilience behavior (Cardoso et al., 2015), these often correspond to operational metrics. To evaluate the effect of collaboration from an operational perspective, we consider the following two indicators that focus on network performance:

$$demand_{loss} = \frac{1}{M} \sum_{m \in M} \frac{demand^{ind}_{loss}(m) - demand^{col}_{loss}(m)}{demand^{ind}_{loss}(m)}, \tag{44}$$

$$cost_{saved} = \frac{1}{M} \sum_{m \in M} \frac{cost^{ind}(m) - cost^{col}(m)}{cost^{ind}(m)}. \tag{45}$$

These metrics measure the impact of collaboration on total cost and demand loss, respectively, when compared to the stand-alone case where each coalition member $m \in M$ operates independently.

Recall that we incorporate a weight for the base scenario in the objective function as its portion to the total number of scenarios in the set N, representing the disruption probability in the network. Figure 5 depicts the effect of different disruption probabilities (10% - 75%) on the network performance under the uniform and gamma distributions for problem size two. It shows that collaboration plays a significant role in improving network performance under disruptions. It indicates the designed ISN meets on average 40% to 100% of the unsatisfied demand in the stand-alone case disruption, while the cost is increased an average of at most 50%. We observe that by increasing the probability of disruption in the resilient ISN, the satisfied demand and cost are decreased. The reason is that there exists more variety of potential disruptions when a higher probability of disruption is considered.

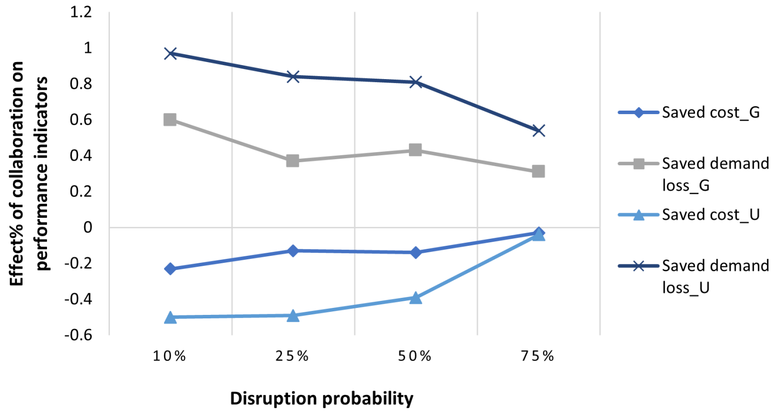

Figure 5: Effect of disruption probability on the network performance (G and U stands for Gamma and uniform distributions, respectively).

We consider four further indicators corresponding to the network design, including node intensity, criticality, flow density, and network complexity.

- *Node intensity:* it is defined as the average of the utilized capacity of each node over its maximum capacity. The utilized capacity is the sum of the flows adjacent to each node.
- *Criticality:* it is assessed by critical nodes in a network. A node is critical when the ratio between the sum of inbound and outbound flows of the node and total flows of the network is greater than a target determined by decision-makers. In these experiments, we consider a 20% target.
- *Density:* it is the ratio between the number of arcs with the actual flow and the total number of arcs in the network.
- *Complexity:* it is evaluated by the number of nodes, products, and partners in a coalition.

Table 3: Network design indicators

Problem size 2	**Gamma distribution**				**Uniform distribution**			
Pobability of disruption scenarios	**10%**	**25%**	**50%**	**75%**	**10%**	**25%**	**50%**	**75%**
Intensity (%)	0.70	0.66	0.67	0.55	0.78	0.59	0.53	0.52
Critical (number)	1.80	2.13	2.51	2.82	1.30	2.50	2.98	3.08
Density (%)	0.15	0.14	0.15	0.15	0.19	0.16	0.15	0.17
Complexity	3 players, 10 products, 65 nodes							

Table 3 shows the effect of the disruption probability on the network design metrics for both the uniform and gamma distributions. It shows that the number of critical nodes increases when increasing the probability of occurrence of disruption scenarios under the uniform and gamma distributions. However, we observe that the intensity of nodes (i.e., used capacity) slightly decreases when increasing the probability of disruption, given that the amount of satisfied demand decreases. Moreover, the probability of disruption seems not to have a major affect on the density rate under both distributions.

The following five metrics are applied from the design perspective to evaluate the impact of collaboration on a resilient network, including intensity, critical and density rates, shared capacity, and capacity expansion with and without collaboration. We say that a node is intense when capacity utilization is over 90%. The intensity rate is the ratio between the number of intense nodes in collaborative and stand-alone cases, that is:

$$Intensity_{rate} = \frac{intense^{ind} - intense^{col}}{intense^{ind}}. \tag{46}$$

Criticality and density rates are also assessed through the same logic as the intensity rate. Shared capacity is the average capacity of facilities shared with others in the coalition. The last indicator is the capacity expansion which is the total capacity extended in ISN and individual supply chains under disruptions. Table 4 presents the design indicators values under different probabilities of disruption considering both the uniform and gamma distributions.

Table 4: Effect of disruption probability on collaboration role in the network design

Problem size 2	**Gamma distribution**				**Uniform distribution**			
Probability of disruption scenarios	**10%**	**25%**	**50%**	**75%**	**10%**	**25%**	**50%**	**75%**
Intensity rate	-1.30	-1.30	-1.20	-0.20	-1.30	-1.10	-0.90	0.02
Criticality rate	0.69	0.70	0.70	0.70	0.72	0.73	0.69	0.68
Density rate	0.70	0.70	0.70	0.69	0.64	0.67	0.71	0.68
Shared capacity	0.35	0.33	0.34	0.25	0.39	0.28	0.35	0.19
Capacity expansion without collaboration	0.11	0.11	0.11	0.12	0.12	0.14	0.11	0.12
Capacity expansion with collaboration	0.02	0.06	0.13	0.15	0.14	0.159	0.19	0.34

From Figure 4, we note an improvement on collaboration in all indicators except the intensity rate. The negative value of intensity rate shows that the number of intense nodes under collaboration is greater than stand-alone case, since incorporating collaboration results in satisfying more demand under disruption, which causes an increase of capacity utilization. In contrast, collaboration results in less critical nodes and density in the network. Besides, we observed that changing the disruption probability does not affect the collaboration impact on the corresponding indicators except the intensity rate. Because there exists a higher variety of potential disruption scenarios when a higher probability of disruption is considered, and consequently, we may face severe disruptions that even a collaborative network cannot be fully resilient.

5.3.2. Disruption Scale

We are also interested in analyzing the effect of disruption scale on the resilience behavior of the network. Therefore, we assess the network of problem size two over different disruption scales ranging from 10% to 100%. For these experiments, we assume a 25% probability of disruption. Table 5 presents the effect of disruption scale on the network performance and design indicators.

This figure shows that the growing disruption scale deteriorates the collaboration impact on the design

Table 5: Effect of the disruption scale on the network performance and design

Problem size 2	**Gamma distribution**				**Uniform distribution**			
Disruption scale	**10%**	**25%**	**50%**	**100%**	**10%**	**25%**	**50%**	**100%**
Intensity rate	-0.67	-1.30	-1.40	-1.80	-0.55	-1.10	-0.90	-1.00
Criticality rate	0.74	0.698	0.65	0.61	0.815	0.73	0.64	0.58
Density rate	0.72	0.70	0.66	-0.04	0.73	0.67	0.67	0.59
Shared capacity	0.30	0.33	0.38	0.34	0.28	0.28	0.37	0.40
Saved cost	-0.10	-0.13	-0.47	-1.90	-0.02	-0.49	-0.59	-0.88
Saved demand loss	0.68	0.37	0.47	0.61	0.96	0.84	0.80	0.55

indicators, including intensity, criticality, density rates, and shared capacity of the network. Figure 6 indicates that a higher cost is required to satisfy almost the same demand by growing the scale of disruption in the network. For instance, under the uniform distribution, the network costs two times more than the stand-alone case to satisfy the demand loss by 61%, when the disruption scale is 100%, while the cost is almost the same as the stand-alone case to improve the same amount of unmet demand when the disruption scale is 10%.

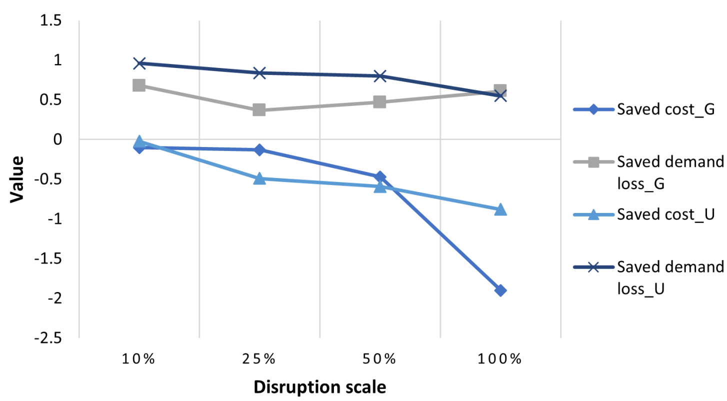

Figure 6: Effect of the disruption scale on the network performance (G and U stands for gamma and uniform distributions, respectively).

5.4. Effects of Flexibility and Complexity on the Resilient Network Performance and Design

We next conduct a sensitivity analysis of the model for different levels of flexibility and complexity of the network. We are interested in observing how different levels of flexibility or complexity affect the ISN resilience behavior in design and performance.

5.4.1. Network Flexibility

We incorporate three resilience strategies simultaneously, including capacity expansion of plants and distribution centers, rerouting, and collaboration. In practice, several challenges and restrictions may not allow players to collaborate at every level of their supply chains. Therefore, we consider different levels of flexibility such that there is a probability for all nodes of the network to be eligible for rerouting or collaboration.

Table 6: Effect of flexibility level on the network design

Problem size 2	**Gamma distribution**				**Uniform distribution**			
flexibility	**25%**	**50%**	**75%**	**100%**	**25%**	**50%**	**75%**	**100%**
Intensity rate	-1.73	-1.65	-1.30	-1.20	-0.96	-0.85	-0.76	-0.64
Criticality rate	0.69	0.68	0.698	0.73	0.77	0.81	0.73	0.80
Density rate	0.66	0.67	0.70	0.71	0.64	0.58	0.67	0.69
Shared capacity	0.37	0.34	0.33	0.32	0.32	0.24	0.28	0.32

Table 6 shows the network design and performance indicator values for different levels of flexibility, ranging from 25% to 100%. We observe that by increasing the flexibility level, the collaboration has a more significant effect on improving the resilience behavior from the performance perspective. However, from the design perspective, it only affects the intensity rate to obtain less intense nodes in the network. Other indicators, including criticality and density rates and shared capacity, are almost the same over different levels of flexibility.

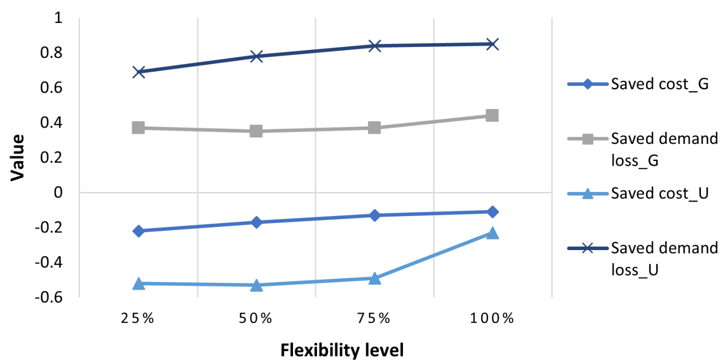

Figure 7: Effect of flexibility on saved demand loss and cost (G and U stands for gamma and uniform distributions, respectively).

Figure 7 depicts the effect of different levels of flexibility on network operational metrics. As expected, by increasing the network flexibility, the saved demand loss and the corresponding cost are improved. We also note that changing the flexibility level has less effect on improving the demand loss under the gamma distribution than the uniform distribution.

5.4.2. Network Complexity

Recall that the complexity of a network is evaluated based on the number of nodes, products, and collaborating players in this paper. Therefore, we order networks by their level of complexity as shown in Table 1. The main challenge in a coalition is establishing a fair collaboration between partners. For this reason, we are interested in evaluating the fairness of collaboration in terms of cost and demand loss between partners by increasing the network complexity. Figure 8 A shows the effect of network complexity on the fairness of collaboration between partners under both the uniform and gamma distributions. In particular, it shows that fairness of demand loss is higher than fairness of the cost between partners over different levels of the network complexity for both distributions.

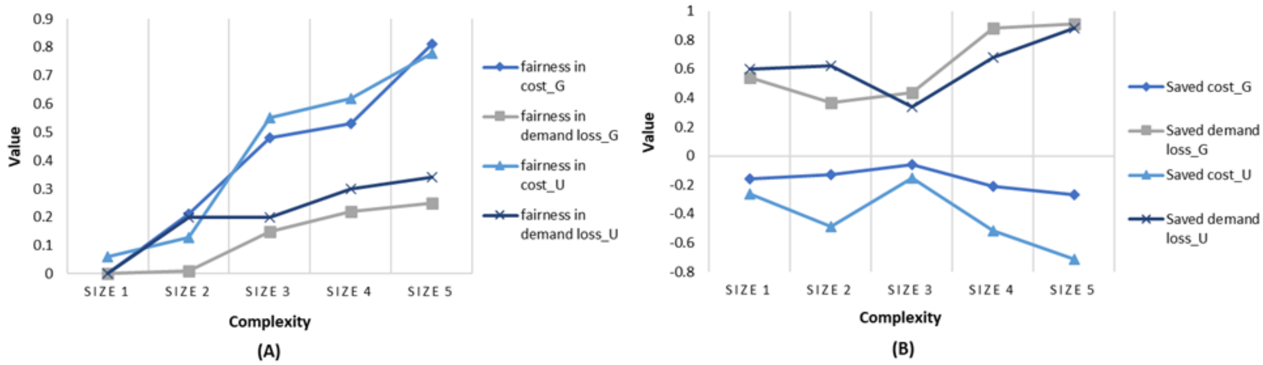

Figure 8: Effect of complexity on fairness of collaboration (A) and performance of the network (B) (G and U stands for gamma and uniform distributions, respectively).

When a network is more complex, it is more challenging to establish fairness between partners. For instance, in problem size one and two, when there are two or three players, the model obtained the optimal solution with less than 10% difference in the improvement of cost or demand loss between players when they are collaborating. The optimal solution of problem size five is less fair since there are six players in the coalition, and the network is much more extensive. Figure 8 B presents the effect of different levels of complexity on the network performance. It shows that collaboration has a more significant effect on network performance when the network is more complex. This figure supports the grand coalition property. Since more partners join a coalition, there are more potential resources to share within the network, which boosts the resilience ability of the network against disruptions.

Figure 9 shows the impact of collaboration on the design of resilient networks with different complexity. We observe that by increasing the complexity, collaboration has a more significant effect on the resilience behaviour of the network from the design perspective. Collaboration in more complex networks resulted in fewer critical nodes, lower density, and more shared capacity between partners in the network under disruption.

The last part of the computational experiments evaluates the performance of the SAA algorithm for different sizes of the problem with up to 117 nodes. Tables 7 and 8 present the summary of the computational results of the SAA algorithm under the gamma and uniform distributions, respectively.

Table 7: Computational results for 10 instances using gamma distribution.

Problem size	**Size 1**	**Size 2**	**Size 3**	**Size 4**	**Size 5**
Mean %GAP	0.11	0.06	-0.017	0.06	0.03
CI at %95	(-0.03 , 0.25)	(-0.15 , 0.27)	(-0.15 , 0.11)	(-0.13 , 0.25)	(-0.16 , 0.20)
SD for %GAP	38660.24	392956.40	346976.47	635992.31	639889.67
Time(minutes)	5.54	25.60	121.70	288.10	899.20

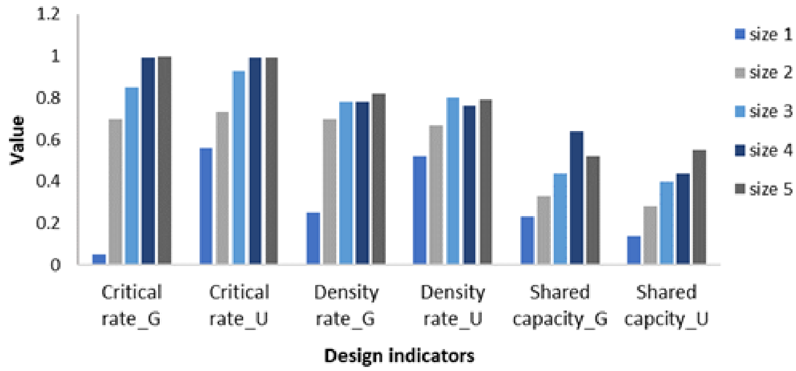

Figure 9: Effect of network complexity on collaboration role in the resilience network design (G and U stands for gamma and uniform distributions, respectively).

Table 8: Computational results for 10 instances using uniform distribution.

Problem size	**Size 1**	**Size 2**	**Size 3**	**Size 4**	**Size 5**
Mean %GAP	0.09	0.01	0.49	0.05	-0.02
CI at %95	(-0.19 , 0.37)	(-0.19 , 0.22)	(0.34 , 0.64)	(-0.11 , 0.21)	(-0.20 , 0.15)
SD for %GAP	74651.09	532693.68	319872.37	535055.94	576401.48
time(minutes)	7.20	13.60	70.01	177.52	331.70

The results of both tables show the efficiency of the SAA algorithm for SCIND. Under both the uniform and gamma distributions, the SAA algorithm always obtained the best solutions with the estimated optimality gaps below 0.10%, except for the problem size three-under uniform distribution with 0.49%. The upper bound of the confidence intervals is always less than 0.38%, except for the same problem with 0.64%. The last observation is that the computational time for the SAA algorithm significantly grows by increasing the size and complexity of the problem.

6. Conclusion

The role of collaboration in the resilience ability of supply chains under disruption has become more visible in recent years. In this paper, we presented a two-stage stochastic optimization framework to design collaborative ISNs under multiple disruptions. We incorporated three different resilience strategies including capacity expansion, capacity sharing, and rerouting. The first-stage decisions determine how much companies have to extend their capacities, and how to form a fair collaboration in terms of the maximum percentage of capacity they will share with others. The second-stage decisions identify the optimal product flows according to the first-stage information and the realized uncertainty scenario. It provides guidelines to collaborate fairly in terms of the amount of capacity shared between partners, and which product flows must be rerouted to improve the resilience against disruptions.

We developed a Monte-Carlo simulation-based algorithm and analyzed the robustness and efficiency of the proposed model on a set of instances with up to 117 nodes and six collaborating companies. The first set of experiments showed the practical convergence of the SAA algorithm under uniform and gamma distributions. The computational experiments on different sizes of instances depicted the efficiency of the applied algorithm under both distributions. It obtained the best solutions with estimated optimality gaps below 0.10% in reasonable computational times. We conducted an extensive sensitivity analysis regarding the role of collaboration on the intertwined supply network performance based on ten different quantitative indicators of the network performance from the design and operational perspectives. The experimental results highlighted the significant role of collaboration in improving the resilience ability of ISNs.

Finally, we would like mention some practical aspects that we have left aside due to space limitations that lead to interesting lines of future research on resilience and collaboration in intertwined supply chain design. For instance, there exist several human-triggered and natural incidents that result in consecutive disruptive events. There may also exist correlation between consecutive disruptions, such that an incident may alter the severity and occurrence probability of potential disruptions in a near future. Therefore, designing a resilient network under consecutive disruptions with unknown probability distributions is an interesting direction of research. In the classical setting of stochastic programs, the stochastic process is independent of decisions made in the system. In practice, there are several cases where decisions affect the remainder of the stochastic process. Incorporating endogenous uncertainty in designing resilient supply network under disruptions is another promising avenue of future research. Considering the effect of decisions such as resilience strategies on the stochastic process of the problem may provide more precise decision tools for designing resilient supply chains.

References

Aggi, 2020. L'economia di guerra ci costa 100 miliardi al mese, dice boccia. URL: `https://www.agi.it/economia/news/2020-03-23/coronavirus-boccia-costo-economia-di-guerra-7773008.Accessed:16.07.2021`.

Azad, N., Davoudpour, H., Saharidis, G.K., Shiripour, M., 2014. A new model to mitigating random disruption risks of facility and transportation in supply chain network design. The International Journal of Advanced Manufacturing Technology 70, 1757–1774.

Bloos, M., Kopfer, H., 2011. On the formation of operational transport collaboration systems, in: Dynamics in Logistics. Springer, pp. 191–201.

Brusset, X., Teller, C., 2017. Supply chain capabilities, risks, and resilience. International Journal of Production Economics 184, 59–68.

Cao, M., Vonderembse, M.A., Zhang, Q., Ragu-Nathan, T., 2010. Supply chain collaboration: conceptualisation and instrument development. International Journal of Production Research 48, 6613–6635.

Cardoso, S.R., Barbosa-Póvoa, A.P., Relvas, S., Novais, A.Q., 2015. Resilience metrics in the assessment of complex supply-chains performance operating under demand uncertainty. Omega 56, 53–73.

Chen, J., Sohal, A.S., Prajogo, D.I., 2013. Supply chain operational risk mitigation: a collaborative approach. International Journal of Production Research 51, 2186–2199.

Christopher, M., Peck, H., 2004. Building the resilient supply chain. International Journal of Logistics Management 15, 1–14.

Cleophas, C., Cottrill, C., Ehmke, J.F., Tierney, K., 2019. Collaborative urban transportation: Recent advances in theory and practice. European Journal of Operational Research 273, 801–816.

Contreras, I., Cordeau, J.F., Laporte, G., 2011. Stochastic uncapacitated hub location. European Journal of Operational Research 212, 518–528.

Cordeau, J.F., Klibi, W., Nickel, S., 2021. Logistics network design, in: Network Design with Applications to Transportation and Logistics. Springer, pp. 599–625.

Cordeau, J.F., Pasin, F., Solomon, M.M., 2006. An integrated model for logistics network design. Annals of Operations Research 144, 59–82.

Craighead, C.W., Blackhurst, J., Rungtusanatham, M.J., Handfield, R.B., 2007. The severity of supply chain disruptions: design characteristics and mitigation capabilities. Decision Sciences 38, 131–156.

Cruijssen, F., Dullaert, W., Fleuren, H., 2007. Horizontal cooperation in transport and logistics: a literature review. Transportation Journal 46, 22–39.

Duong, L.N.K., Chong, J., 2020. Supply chain collaboration in the presence of disruptions: a literature review. International Journal of Production Research 58, 3488–3507.

Fattahi, M., Govindan, K., Keyvanshokooh, E., 2017. Responsive and resilient supply chain network design under operational and disruption risks with delivery lead-time sensitive customers. Transportation Research Part E: Logistics and Transportation Review 101, 176–200.

Frisk, M., Göthe-Lundgren, M., Jörnsten, K., Rönnqvist, M., 2010. Cost allocation in collaborative forest transportation. European Journal of Operational Research 205, 448–458.

Gholami-Zanjani, S.M., Klibi, W., Jabalameli, M.S., Pishvaee, M.S., 2020. The design of resilient food supply chain networks prone to epidemic disruptions. International Journal of Production Economics 233, 108001.

Goemans, M.X., Skutella, M., 2004. Cooperative facility location games. Journal of Algorithms 50, 194–214.

Goldbeck, N., Angeloudis, P., Ochieng, W., 2020. Optimal supply chain resilience with consideration of failure propagation and repair logistics. Transportation Research Part E: Logistics and Transportation Review 133, 101830.

Govindan, K., Fattahi, M., Keyvanshokooh, E., 2017. Supply chain network design under uncertainty: A comprehensive review and future research directions. European Journal of Operational Research 263, 108–141.

Guo, Y., Yu, J., Allaoui, H., Choudhary, A., 2022. Lateral collaboration with cost-sharing in sustainable supply chain optimisation: A combinatorial framework. Transportation Research Part E: Logistics and Transportation Review 157, 102593.

Hasani, A., Khosrojerdi, A., 2016. Robust global supply chain network design under disruption and uncertainty considering resilience strategies: A parallel memetic algorithm for a real-life case study. Transportation Research Part E: Logistics and Transportation Review 87, 20–52.

Hendricks, K.B., Singhal, V.R., 2005. An empirical analysis of the effect of supply chain disruptions on long-run stock price performance and equity risk of the firm. Production and Operations Management 14, 35–52.

Hosseini, S., Ivanov, D., Dolgui, A., 2019. Review of quantitative methods for supply chain resilience analysis. Transportation Research Part E: Logistics and Transportation Review 125, 285–307.

Ivanov, D., Dolgui, A., 2020. Viability of intertwined supply networks: extending the supply chain resilience angles towards survivability. a position paper motivated by covid-19 outbreak. International Journal of Production Research 58, 2904–2915.

Ivanov, D., Pavlov, A., Dolgui, A., Pavlov, D., Sokolov, B., 2016. Disruption-driven supply chain (re)-planning and performance impact assessment with consideration of pro-active and recovery policies. Transportation Research Part E: Logistics and Transportation Review 90, 7–24.

Kim, Y., Chen, Y.S., Linderman, K., 2015. Supply network disruption and resilience: A network structural perspective. Journal of Operations Management 33, 43–59.

Kleywegt, A.J., Shapiro, A., Homem-de Mello, T., 2002. The sample average approximation method for stochastic discrete optimization. SIAM Journal on Optimization 12, 479–502.

Klibi, W., Martel, A., 2012. Modeling approaches for the design of resilient supply networks under disruptions. International Journal of Production Economics 135, 882–898.

Klibi, W., Martel, A., Guitouni, A., 2010. The design of robust value-creating supply chain networks: a critical review. European Journal of Operational Research 203, 283–293.

Li, Y., Zobel, C.W., Seref, O., Chatfield, D., 2020. Network characteristics and supply chain resilience under conditions of risk propagation. International Journal of Production Economics 223, 107529.

Mak, W.K., Morton, D.P., Wood, R.K., 1999. Monte carlo bounding techniques for determining solution quality in stochastic programs. Operations Research Letters 24, 47–56.

Martel, A., Klibi, W., 2016. Designing value-creating supply chain networks. Springer, New York.

Miller-Hooks, E., Zhang, X., Faturechi, R., 2012. Measuring and maximizing resilience of freight transportation networks. Computers & Operations Research 39, 1633–1643.

Pettit, T.J., Croxton, K.L., Fiksel, J., 2013. Ensuring supply chain resilience: development and implementation of an assessment tool. Journal of Business Logistics 34, 46–76.

Santoso, T., Ahmed, S., Goetschalckx, M., Shapiro, A., 2005. A stochastic programming approach for supply chain network design under uncertainty. European Journal of Operational Research 167, 96–115.

Shapiro, A., Homem-de Mello, T., 1998. A simulation-based approach to two-stage stochastic programming with recourse. Mathematical Programming 81, 301–325.

Shapley, L.S., 1953. A value for n-person games. Contributions to the Theory of Games 2, 307–317.

Shekarian, M., Mellat Parast, M., 2020. An integrative approach to supply chain disruption risk and resilience management: A literature review. International Journal of Logistics Research and Applications 24, 1–29.

Simatupang, T.M., Sridharan, R., 2002. The collaborative supply chain. The International Journal of Logistics Management 13, 15–30.

Snyder, L.V., Atan, Z., Peng, P., Rong, Y., Schmitt, A.J., Sinsoysal, B., 2016. OR/MS models for supply chain disruptions: A review. IIE Transactions 48, 89–109.

Torabi, S., Baghersad, M., Mansouri, S., 2015. Resilient supplier selection and order allocation under operational and disruption risks. Transportation Research Part E: Logistics and Transportation Review 79, 22–48.

Verdonck, L., Beullens, P., Caris, A., Ramaekers, K., Janssens, G.K., 2016. Analysis of collaborative savings and cost allocation techniques for the cooperative carrier facility location problem. Journal of the Operational Research Society 67, 853–871.

Wang, Y., Ma, X., Liu, M., Gong, K., Liu, Y., Xu, M., Wang, Y., 2017. Cooperation and profit allocation in two-echelon logistics joint distribution network optimization. Applied Soft Computing 56, 143–157.